

Lawrence Berkeley National Laboratory

Recent Work

Title

CROSSED BEAM STUDIES OF ENDOERGIC BIMOLECULAR REACTIONS: PRODUCTION OF STABLE TRIHALOGEN RADICALS

Permalink

<https://escholarship.org/uc/item/6997d2kr>

Author

Valentini, James J.

Publication Date

1976-04-01

U U J 4 4 U 7 3 1 9
To be presented at the September 1976
Faraday Discussion on Potential Energy
Surfaces, University of Sussex,
Brighton, England, September 8 - 10, 1976

LBL-4543
c.1

CROSSED BEAM STUDIES OF ENDOERGIC BIMOLECULAR
REACTIONS: PRODUCTION OF STABLE TRIHALOGEN RADICALS

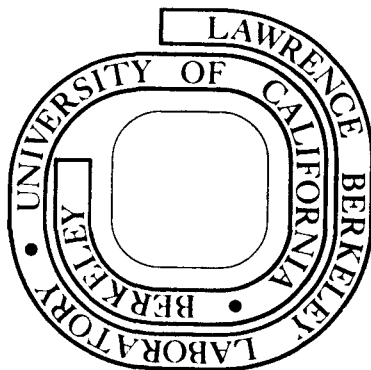
James J. Valentini, Michael J. Coggiola, and Yuan T. Lee

April 1976

Prepared for the U. S. Energy Research and
Development Administration under Contract W-7405-ENG-48

For Reference

Not to be taken from this room



LBL-4543
c.1

DISCLAIMER

This document was prepared as an account of work sponsored by the United States Government. While this document is believed to contain correct information, neither the United States Government nor any agency thereof, nor the Regents of the University of California, nor any of their employees, makes any warranty, express or implied, or assumes any legal responsibility for the accuracy, completeness, or usefulness of any information, apparatus, product, or process disclosed, or represents that its use would not infringe privately owned rights. Reference herein to any specific commercial product, process, or service by its trade name, trademark, manufacturer, or otherwise, does not necessarily constitute or imply its endorsement, recommendation, or favoring by the United States Government or any agency thereof, or the Regents of the University of California. The views and opinions of authors expressed herein do not necessarily state or reflect those of the United States Government or any agency thereof or the Regents of the University of California.

CROSSED BEAM STUDIES OF ENDOERGIC BIMOLECULAR REACTIONS:
PRODUCTION OF STABLE TRIHALOGEN RADICALS

(i)

James J. Valentini, Michael J. Coggiola and Yuan T. Lee

(ii)

Lawrence Berkeley Laboratory and Department of Chemistry
The University of California, Berkeley, California 94720

(iii)

Lawrence Berkeley Laboratory, Building 70A
The University of California
Berkeley, California 94720
Attn: Michael J. Coggiola

(iv)

12

(v)

Trihalogen Radicals

ABSTRACT

The trihalogens IIF and ClIF and the pseudo-trihalogen HIF have been directly observed as the products of the endoergic bimolecular reactions of F_2 with I_2 , ICl and HI in a crossed molecular beam experiment. At high collision energies a second reactive channel producing IF becomes important. Product angular and velocity distributions show that this IF does not result from a four-centre exchange reaction. Observed threshold energies for the formation of IIF, ClIF and HIF yield lower bounds on the stability of these molecules (with respect to the separated atoms) of 69, 81 and 96 kcal/mole, respectively. Analysis of the product centre-of-mass angular distributions indicate that a slightly non-linear approach is most effective in bringing about reaction to form the stable triatomic radical. These studies reveal a potentially important mechanism for the $F_2 + I_2 \rightarrow 2IF$ bulk gas phase reaction.

The understanding of reaction dynamics from the features of a potential energy surface has improved significantly in recent years. For a simple system, such as $F + H_2$, accurate ab initio calculations have become possible,¹ and the experimentally observed product angular² and energy distributions³ can be explained satisfactorily. For many complicated systems, one does not expect to be able to calculate the potential energy hypersurface as accurately, but if there are certain dominant features, then the reaction dynamics can still be understood without detailed information about the hypersurface. One example is the formation of long lived "collision complexes," such as $F + C_2H_2Cl_2 \rightarrow C_2H_2Cl_2F^\ddagger$.⁴ The dynamics of product formation will be dominated by statistical features of the decomposition of the collision complex.

There are many simple reactions involving heavy atoms, such as $F + I_2 \rightarrow IF + I$, for which reliable potential energy surface calculation is quite difficult, and for which there is no reason to believe the statistical theory will be applicable. Important features of the potential energy surface for these cases are often inferred at present from experimental observation rather than the other way around. Actually, all three systems mentioned above have similar exoergicities, ~30 kcal, and the differences in the potential energy surface along the reaction coordinate which are responsible for such drastic differences in reaction dynamics are shown schematically in Figure 1. The surface for $F + I_2 \rightarrow IF + I$ drawn here is derived from qualitative observation in previous crossed molecular beam experiments.⁵ The observed near

forward-backward symmetry in the angular distribution and the extremely high vibrational excitation of the IF molecule indicate that the potential energy surface must be an early downhill attractive surface with a "sticky" I_2F intermediate.

The stability of the I_2F reaction intermediate is of great interest and importance. Whether the potential energy of I_2F lies slightly above or below the product $IF + I$, may not be very important in the general understanding of the reaction dynamics of the very exoergic $F + I_2 \rightarrow IF + I$ reaction. However, whether I_2F is a chemically stable species or just an unstable transient in the $F + I_2$ reaction is extremely important in the understanding of the macroscopic reaction mechanism and energy pathways of the reaction involving F_2 and I_2 .⁶ There have been several discussions on the stability of these trihalogen systems in the past, based on molecular orbital theory,⁷ the dynamics of atom-molecule exchange reactions,⁸ and termolecular recombination studies.⁹ The observation of trihalogen radical molecules in matrix isolation experiments has been reported in the past,¹⁰ but the direct gas phase, mass spectrometric identification has only very recently been made in our laboratory.¹¹

There are two different approaches one can take using the crossed molecular beam method for deriving information about the stability of collision complexes. One approach attempts to infer information about complex stability by investigating the lifetime of the complex. In a crossed molecular beam experiment the rotational period of the complex can be conveniently used as a clock, since the product angular distri-

bution displays forward-backward symmetry only if the lifetime of the complex is longer than one rotational period.¹² By adjusting collision energies in the reaction of $F + CH_3I$, it has been shown¹³ that the lifetime of the complex can be adjusted to match the rotational period. Once the lifetime of the complex is estimated from the evaluation of the rotational period, one can use statistical theory and information on the exoergicities of the chemical reactions to calculate the stability of the complexes. The stability of CH_3IF estimated by this method is quite close to a value obtained by the synthetic method¹⁴ outlined below. However, the applicability of this method depends on the successful matching of the rotational period and the lifetime of the complex, and the validity of statistical theory in describing the decomposition of the collision complex. The former is not easily accomplished experimentally for most of the systems, and the latter may not obtain, especially at high collision energies.

The second method, which we used in this work, involves the direct synthesis of the radical molecules in question through endoergic molecule-molecule reactions,¹⁴ such as $F_2 + I_2 \rightarrow I_2F + F$. By adjusting collision energies, the threshold energy of formation of the radical molecules can be obtained, and this in turn provides a lower bound on the binding energy of the radical molecules. In this paper, we will discuss the energetics of a series of radical molecules, I_2F , $ClIF$ and HIF , obtained by the molecular beam synthetic method; the dynamics of the molecule-molecule reactions of F_2 with I_2 , ICl and HI ; and the important role I_2F might play in the mechanism and energy pathways in macroscopic reactions involving F_2 and I_2 .

Experimental

The crossed molecular beam apparatus employed in these experiments has been described in detail elsewhere.¹⁵ Both reactant beams were generated by supersonic expansion using differentially pumped beam sources. Mixtures of molecular fluorine (1-2%) in He or He/Ne carrier gases were used to vary the collision energy. Additional control of the fluorine beam energy was provided by a resistance heated nickel oven operated between 300 and 900 K, without appreciable F atom production. The I₂ and ICl beams were produced using 10-15% mixtures of the halogens in Ar, while the HI beam was generated without use of a carrier gas. A glass nozzle maintained at a constant temperature (300-400 K) was used to fix the energy of these beams. This arrangement resulted in a range of collision energies from 3 to 20 kcal/mole, with a spread in energy of $\pm 25\%$. Product molecules were detected in the plane of the reactant beams using a rotatable quadrupole mass spectrometer equipped with an electron bombardment ionizer utilizing ion counting techniques. In addition to the measurement of the angular distribution of the products, the product velocity distributions were also determined by means of cross correlation time-of-flight¹⁶ using on-line computer control and data reduction. This technique provided a velocity resolution of better than 10%.

Angular distribution data were obtained using counting times between 40 and 100 seconds for each point, and periodically returning to a reference angle to provide long-term normalization. Plotted angular distributions represent the average of several separate scans.

Time-of-flight data were recorded for 15 to 45 minutes depending on the signal level. All velocity distributions were converted from the measured number density to laboratory flux with corrections for the shutter function and finite ionizer length. Product angular and velocity distributions were measured in this way for several collision energies. In addition, separate experiments were carried out to accurately determine the energy threshold for product formation.

Results and Analysis

Any attempt to observe the trihalogen species XIF as a product of the endoergic reaction of F_2 and XI,



will only be successful if reaction (1) is less endoergic than the reaction



that is, if XIF decomposition into IF and X is endoergic; and provided that the four-centre exchange mechanism does not dominate. The present investigation shows that above threshold energies of 4, 6, and 11 kcal/mole respectively collisions between F_2 and XI (X = I, Cl, H) do produce principally XIF and F as in (1). As the collision energy is increased reaction (2) becomes important, first for $F_2 + I_2$, and later for $F_2 + ICl$ also, but not for $F_2 + HI$ at the collision energies used here.

Angular distributions of both I_2F (m/e 273) and IF (m/e 146) products of the $F_2 + I_2$ reaction at two collision energies are shown in Figure 2. In each case, part of the measured IF^+ signal resulted from break-up of I_2F in the detector ionizer, hence a fraction of the I_2F signal has been subtracted from the IF signal, and the corrected IF angular distributions are also shown. The correction factor was determined from the fractionation ratio, $I_2F^+ : IF^+$, of I_2F produced at collision energies at which IF is not expected to form directly. Here $I_2F^+ : IF^+$ was ~2.0 for 200 eV ionizing electrons.

Figure 3 shows the corresponding angular distributions of ClIF (m/e 181, $Cl^{35}IF$) and IF from the $F_2 + ICl$ reaction. Corrections to the IF signal for ClIF fractionation have been made as for I_2F/IF . The

ClIF fractionation ratio, $\text{ClIF}^+:\text{IF}^+$, was ~ 1.0 under these conditions. Although the reactive channel $\text{F}_2 + \text{ICl} \rightarrow \text{Cl} + \text{IF} + \text{F}$ is energetically inaccessible (19 kcal/mole endoergic) at the nominal collision energies indicated, there are F_2/ICl collisions involving F_2 molecules from the high velocity tail of the supersonic velocity distribution ($\pm 20\%$ spread in energy) which are sufficiently energetic to produce IF. That this channel is open can be seen from the corrected (for ClIF fractionation) IF distributions of Figure 3.

No IF distributions are shown in Figure 4 for the $\text{F}_2 + \text{HI}$ system, as the reactive channel (2) producing IF is prohibitively endoergic (41 kcal/mole). Some IF^+ was produced by ionizer fractionation, as determined from an investigation at high mass resolution, but the angular distributions shown were taken with less than unit mass resolution and represent the sum of the HIF^+ (m/e 147) and IF^+ (m/e 146) signals.

It is important to note that for the $\text{F}_2 + \text{ICl}$ system there were no peaks in the mass spectrum at m/e 56 (Cl^{37}F) or m/e 54 (Cl^{35}F). In addition, for $\text{F}_2 + \text{HI}$ no peak at m/e 20 (HF) was observed. This strongly suggests that the observed products are indeed ClIF and HIF, with the F atom attached to I, not to Cl or H as IClF or HIF. This is in agreement with the unfailingly regular pattern of nuclear arrangements in triatomic ABC systems, which always have the least electronegative atom of the three at the middle position of the molecule. For all molecules with more than twelve valence electrons this general conclusion follows from the fact that the charge distribution of the π orbitals is generally more concentrated at the terminal atoms than at the center of the molecule.

These results indicate the $F_2 + XI$ reaction does not proceed via a highly exoergic four-centre exchange mechanism to produce XF and IF. For $F_2 + ICl$ and $F_2 + HI$ no ClF or HF products were detected. For $F_2 + I_2$ the four-centre exchange produces only IF, but this mechanism is exoergic by more than 60 kcal/mole. If even a relatively small fraction of this energy appeared as product translation, the IF angular distributions would be much broader. Also, since the four-centre exchange mechanism does produce two identical molecules, the product distributions would have forward-backward symmetry in the centre-of-mass coordinate system, and be roughly symmetric about the centre-of-mass angle in the laboratory under our experimental conditions.

From the angular distributions shown and from time-of-flight velocity analysis of the products, centre-of-mass contour maps of product flux have been constructed. These are shown in Figures 5, 6, and 7.

These contour maps of $I_{c.m.}(\theta, u)$, the centre-of-mass doubly differential reactive scattering cross section, were constructed by iterative deconvolution of the measured $\bar{I}_{LAB}(\theta, v)$ cross section data, using a modified version of a computer method due to Siska.¹⁷ This technique solves the equation:

$$\bar{I}_{LAB}(\theta, v) = \sum_i f_i \frac{v^2}{u_i^2} I_{c.m.}(\theta_i, u_i) \quad (3)$$

iteratively for $I_{c.m.}(\theta, u)$. The summation is taken over the range of transformation Newton diagrams generated by the finite widths of the beam velocity distributions and angular spreads, and f_i is the

weighting factor for the i^{th} Newton diagram. Quantities with a bar indicate beam velocity and intersection angle averaged quantities.

By assuming that the monochromatic $I_{\text{c.m.}}(\theta, u)$ is related to a monochromatic $I_{\text{LAB}}(\theta, v)$ by a single "canonical" Newton diagram:

$$I_{\text{LAB}}(\theta, v) = \frac{v^2}{u^2} I_{\text{c.m.}}(\theta, u), \quad (4)$$

equation (3) becomes:

$$\bar{I}_{\text{LAB}}(\theta, v) = \sum_i f_i \frac{v_i^2}{v_i} I_{\text{LAB}}(\theta_i, v_i). \quad (5)$$

The initial guess for I_{LAB} is just the experimental distribution, $\bar{I}_{\text{LAB}}^{\text{EXPT}}$. Corrections to I_{LAB} are then generated by a ratio method, i.e.:

$$I_{\text{LAB}}^{(0)} = \bar{I}_{\text{LAB}}^{\text{EXPT}} \quad (6)$$

$$I_{\text{LAB}}^{(n+1)} = I_{\text{LAB}}^{(n)} \cdot (\bar{I}_{\text{LAB}}^{\text{EXPT}} / \bar{I}_{\text{LAB}}^{(n)}). \quad (7)$$

The iteration is repeated until $\bar{I}_{\text{LAB}}^{\text{EXPT}} / \bar{I}_{\text{LAB}}^{(n)} \approx 1$. This technique allows the "ideal" monochromatic centre-of-mass distribution to be obtained without any assumption about the functional form of the distribution.

For substantially endoergic reactions at collision energies not far in excess of the threshold, the reactive cross section is expected to be quite strongly dependent on the collision energy. This is certainly the case for the reactions studied here. In the case of $\text{F}_2 + \text{I}_2$ and $\text{F}_2 + \text{ICl}$ the energy dependence of the cross section for production of I_2F or ClIF is complicated by the presence of a second

reactive channel, that which results in IF production. In order to obtain a centre-of-mass distribution which would accurately reproduce the experimental data it was necessary to weight the Newton diagrams according to the energy dependence of the reactive cross sections. Hence, equation (5) becomes:

$$\bar{I}_{\text{LAB}}(\theta, v) = \sum_i f_{E_i} f_{v_i} \frac{v_i^2}{v_1} I_{\text{LAB}}(\theta, v_i). \quad (8)$$

The cross section energy dependence used in fitting all three systems was similar, namely a very rapid rise from threshold with increasing collision energy, gradually tapering off to a near plateau. The energy dependence was partly determined from experimental relative cross section measurements. However, in energy regions for which the experimental measurement was not made or was insufficiently detailed, adjustments or extrapolations of the experimental energy dependence data were made. The adjustments and extrapolations were chosen so as to give an accurate fit to the experimental angular and velocity data, i.e. $\bar{I}_{\text{LAB}}(\theta, v)$, and so as to be physically consistent, that is to give a smoothly varying cross section energy dependence in good agreement with the experimental relative cross section data.

This energy weighting makes the most probable Newton diagram somewhat larger (~5%) than that which maximizes the quantity:

$$(v_1^2 + v_2^2)^{1/2} n_1(v_1) n_2(v_2), \quad (9)$$

the product of the relative velocity and the number densities of the two beams. This larger N.D. is used as the "canonical" one (equation

(4)) for the deconvolution. This energy weighting also makes the most probable collision energy somewhat larger (~10%) than the nominal collision energies, also derived from the maximum in equation (9), given in the figures.

The experimental data and laboratory data calculated from the deconvoluted centre-of-mass flux distributions are compared in Figures 8 and 9. The fit to the lab angular distributions and I_2F lab velocity distributions are quite good. Fits to the ClIF and HIF velocity distributions, not shown, are equally satisfactory.

The centre-of-mass contour maps show the sharply forward peaked nature of the XIF products. It is significant that the I_2F distribution is considerably narrower in recoil velocity than either the ClIF or HIF products. In part this is a consequence of the more restrictive kinematics of the $I_2F + F$ system, for which the detected product is more than 14 times the mass of the other. However, it is also indicative of a "thermodynamic" constraint of the products to large recoil velocity (energy) due to the low stability of I_2F with respect to $I + IF$. This thermodynamic constraint allows formation of the trihalogen only when the excess energy channeled into translation of products is such that internal excitation of I_2F is not sufficient to dissociate it into IF and I. This behavior is evident in the I_2F lab angular distributions of Figure 2, which show only slight variation in going from 9.6 kcal/mole collision energy (~5.6 kcal/mole excess energy) to 12.9 kcal/mole collision energy (~8.9 kcal/mole excess energy). No such constraint exists, at the collision energies studied, for either ClIF or HIF and

this is reflected in both the centre-of-mass contour maps and lab angular distributions.

The thermodynamic constraint of the I_2F/F recoil energy distribution is even more clearly evident in Figure 10, which gives the intensity, $P(E_T')$, versus recoil energy, E_T' , i.e. $\sum_{\theta} I_{c.m.}(\theta, E_T')$ where $I_{c.m.}(\theta, E_T') \propto I_{c.m.}(\theta, u)/u$, for the systems studied. The I_2F/F distribution is much more sharply peaked than that for ClIF/F or HIF/F and peaks at an energy which represents a much larger fraction of the available energy than the ClIF/F distribution. The average product translational energy,

$$\overline{E_T'} = \frac{\sum_{E_T'} P(E_T') \cdot E_T'}{\sum_{E_T'} P(E_T')},$$

is ~30% of the total available energy for ClIF production, while for the $I_2F + F$ products more than 50% (5.1 kcal/mole) of the available energy appears in translation. For HIF production the average energy in translation is again high, 2.8 kcal/mole, ~47%. Any such comparison of product translational energies must of course recognize the rather substantial change in the reaction kinematics in changing the F atom abstracting species from I_2 to ICl to HI. However, the $F_2 + I_2$ and $F_2 + ICl$ systems would seem to be similar enough kinematically to allow one to attribute the recoil energy distribution differences to the operation of this thermodynamic constraint.

It is clear that the increased sharpness of the I_2F lab angular distributions relative to those for ClIF and HIF is due to the sharpness

in recoil velocity (energy) and not in recoil angle. This can be seen in Figure 11, which shows the centre-of-mass angular distributions, where $I(\theta) = \sum_{E_T'} I_{\text{c.m.}}(\theta, E_T')$. The I_2F distribution is actually broader ($\sim 30^\circ$ HWHM) than either the HIF or ClIF distributions ($\sim 15^\circ$ HWHM). It is not clear whether the relative broadness of the I_2F distribution is dynamically significant or merely a consequence of the more unfavorable kinematics of the I_2F/F system which makes ratio method deconvolution of the centre-of-mass distribution more difficult.

Discussion

The stabilities of the XIF species ($X = I, Cl, CH_3, H$) have been derived from the experimentally measured thresholds for the reactions: $F_2 + XI \rightarrow XIF + F$, and the known¹⁸ F_2 and XI dissociation energies. Figure 12 gives an energy schematic for the trihalogens and pseudo-trihalogen discussed. It is interesting to note that I_2F is only 3 kcal/mole more stable than $I + IF$. The stability of this radical is due primarily to the strength of the II-F bond. As the terminal atom (group) in XIF is changed through the sequence I, Cl, CH_3 , H the trihalogen stability increases due to an increase in the X-IF bond strength, a reflection of the increased X-I diatomic (polyatomic) bond strength. Indeed, when $X=H$ the stability of the pseudo-trihalogen is due more to the H-IF bond than to the HI-F bond.

The very sharply forward peaked distributions for all three systems would seem to indicate a preference for a bent geometry for F atom abstraction by XI, that is a preference for an F-F-I angle or F-I-X angle of less than 180° in F-F-I-X. When $X=H$ the mass of X is negligible in comparison with I, and the F-I-X angle will not be an important determinant of the product angular distribution. The forward peaking of HIF is thus a consequence of the bent F-F-I angle. Of course high energy collisions tend to favor forward peaking, and it is important to note that the IF produced in the $I + F_2$ reaction, kinematically identical to the $HI + F_2$ system, is backward peaked at thermal energies,¹⁹ indicating that the bending angle of F-F-I must not be very large. The forward scattering of HIF observed in this work, in contrast to the

backward peaking of IF from $I + F_2$, can be attributed to the difference in collision energy rather than to a larger bending angle for F-F-IH compared to F-F-I.

For $X = I$ or Cl the mass of X is no longer negligible in comparison with I and both the F-F-I and F-I-X angles will be important. For the $F_2 + I_2$ and $F_2 + ICl$ systems backward scattering of FIX is only possible if all four atoms are aligned collinearly in the critical configuration. The observed forward peaking of FIX clearly argues against such a geometry, favoring bending of one or both of F-F-I and F-I-X. Simple molecular orbital considerations²⁰ lead one to expect the F-F-I and F-I-X angles to be quite similar, so it is likely that both F-F-I and F-I-X are slightly bent.

There are no ABC molecules with 21 valence electrons whose molecular geometry is exactly known, so it is somewhat difficult to precisely predict a preference for a particular F-F-I or F-I-X angle, nor can an unambiguous answer be determined from a simple M.O. picture. However, ClF_2 is thought to have a bond angle $\sim 145^\circ$.^{7,10} All known triatomic molecules with 20 valence electrons are bent ($\sim 100^\circ$ bond angle), and those with 22 electrons are linear. It is thus not inconsistent to expect a bent F-F-I and F-I-X geometry in $F_2 + XI$ reactions.

The potentially important role played by stable radicals in promoting bimolecular chemical reactions such as $F_2 + XI$ had not been suspected previously. The fact that a fluorine atom, which can initiate a chain reaction in F_2/XI mixtures, can be generated in a collision between F_2 and XI through reaction (1) at a relative kinetic energy as low as

4 kcal/mole (for $F_2 + I_2$) is intriguing. This is especially so considering that 37 kcal/mole is necessary to dissociate F_2 and at least 37 kcal/mole to dissociate XI.

The threshold energy of reaction (2), which also produces an F atom, as well as an X atom, can be calculated from bond dissociation energies¹⁸ and is 7 kcal/mole, 19 kcal/mole, and 41 kcal/mole for $X = I, Cl, \text{ and } H$ respectively. For the $F_2 + I_2$ and $F_2 + ICl$ systems these energies are also smaller than the F_2 or XI bond dissociation energies. Even if XIF production by reaction (1) is not important, reaction (2) could be a significant source of F and X atoms in F_2/XI mixtures.

The results presented here have an important bearing on the interpretation of the results of a recent study⁶ of the gas phase kinetics of the F_2/I_2 system. If I_2F were not stable, and consequently of no significance in the F_2/I_2 reaction mechanism, the only exoergic source of IF in F_2/I_2 mixtures would be the $F + I_2$ and $I + F_2$ reactions, since IF_2 is not expected to be stable and was not observed in this work. Each of these reactions is ~30 kcal/mole exoergic, insufficiently exoergic to be responsible for the IF chemiluminescence observed⁶ in F_2/I_2 mixtures. However, since I_2F is stable, another exoergic IF producing channel is open, namely the reaction



This reaction is exoergic by 64 kcal/mole, and the IF chemiluminescence observed may be due exclusively to the operation of reaction (10).

0 0 0 0 4 4 0 7 3 3 0

-17-

This work is supported by the U. S. Office of Naval Research and
U. S. Energy Research and Development Administration.

REFERENCES

1. C. F. Bender, P. K. Pearson, S. V. O'Neil and H. F. Schaefer, J. Chem. Phys., 1972, 56, 4626.
2. T. P. Schafer, Ph.D. Thesis (University of Chicago, Chicago, Illinois, 1973).
- 3a. M. J. Berry, J. Chem. Phys., 1973, 59, 6229.
- b. J. C. Polanyi and K. B. Woodall, J. Chem. Phys., 1972, 57, 1574.
- c. J. H. Parker and G. C. Pimentel, J. Chem. Phys., 1969, 51, 91.
4. K. Shobatake, S. A. Rice and Y. T. Lee, J. Chem. Phys., 1973, 59, 12.
5. Y. C. Wong and Y. T. Lee, Disc. Faraday Soc., 1973, 55, 383.
6. J. W. Birks, S. D. Gabelnick and H. S. Johnston, J. Mol. Spectr., 1975, 57, 23.
- 7a. S. D. Peyerimhoff and R. J. Buenker, J. Chem. Phys., 1968, 49, 2473.
- b. R. J. Buenker and S. D. Peyerimhoff, Chem. Rev., 1974, 74, 125.
- c. S. R. Ungemach and H. F. Schaefer, J. Amer. Chem. Soc., 1976, 98, 1658.
- 8a. Y. T. Lee, J. D. McDonald, P. R. LeBreton and D. R. Herschbach, J. Chem. Phys., 1968, 49, 2447.
- b. Y. T. Lee, P. R. LeBreton, J. D. McDonald and D. R. Herschbach, J. Chem. Phys., 1969, 51, 455.
9. D. L. Bunker and N. Davidson, J. Amer. Chem. Soc., 1958, 80, 5090.
- 10a. L. Y. Nelson and G. C. Pimentel, J. Chem. Phys., 1967, 47, 3671.
- b. G. Mamantov, E. J. Vasini, M. C. Moulton, D. G. Vickroy and T. Maekawa, J. Chem. Phys., 1971, 54, 3419.

11. J. J. Valentini, M. J. Coggiola and Y. T. Lee, *J. Amer. Chem. Soc.*, 1976, 98, 853.
12. W. B. Miller, S. A. Safron and D. R. Herschbach, *Disc. Faraday Soc.*, 1967, 44, 108.
13. J. M. Farrar and Y. T. Lee, *J. Chem. Phys.*, 1975, 63, 3639.
14. J. M. Farrar and Y. T. Lee, *J. Amer. Chem. Soc.*, 1975, 96, 7570.
15. Y. T. Lee, J. D. McDonald, P. R. Lebreton and D. R. Herschbach, *Rev. Sci. Instr.*, 1969, 40, 1402.
16. V. L. Hirschy and J. P. Aldridge, *Rev. Sci. Instr.*, 1971, 42, 381.
17. P. E. Siska, *J. Chem. Phys.*, 1973, 59, 6052.
- 18a. J. Berkowitz and A. C. Wahl, *Adv. Flourine Chem.*, 1973, 7, 147.
 - b. B. Darwent, *Bond Dissociation Energies in Simple Molecules*, National Bureau of Standards, Washington, 1970, NSRD-NBS-31.
19. Y. C. Wong, unpublished.
20. A. P. Walsh, *J. Chem. Soc.*, 1953, 2266.

FIGURES

Fig. 1. -- Idealized representation of the potential energy curves for the reactions $F + H_2$, I_2 and $C_2H_2Cl_2$.

Fig. 2. -- ● Experimental laboratory angular distribution of IF produced in the reaction $F_2 + I_2$ at collision energies of 12.9 and 9.7 kcal/mole; ◇ experimental laboratory angular distribution of I_2F produced in the same reaction; ○ IF angular distribution connected for I_2F^+/IF^+ fractionation, see text.

Fig. 3. -- ● Experimental laboratory angular distribution of IF produced in the reaction $F_2 + ICl$ at collision energies of 17.4 and 16.1 kcal/mole; ◇ experimental laboratory angular distribution of ClIF produced in the same reaction; ○ IF angular distribution connected for $ClIF^+/IF^+$ fractionation, see text.

Fig. 4. -- ● Experimental laboratory angular distribution of HIF produced in the reaction $F_2 + HI$ at collision energies of 16.1 and 14.9 kcal/mole.

Fig. 5. -- Contour map of I_2F flux density in the centre-of-mass coordinate system produced in the reaction $F_2 + I_2$ at a collision energy of 12.9 kcal/mole. These contours were obtained by fitting the experimental laboratory angular and velocity distributions.

Fig. 6. -- Contour map of ClIF flux density in the centre-of-mass coordinate system produced in the reaction $F_2 + ICl$ at a collision energy of 17.4 kcal/mole. These contours were obtained by fitting the experimental laboratory angular and velocity distributions.

Fig. 7. -- Contour map of HIF flux density in the centre-of-mass coordinate system produced in the reaction $F_2 + HI$ at a collision energy of 16.1 kcal/mole. These contours were obtained by fitting the experimental laboratory angular and velocity distributions.

Fig. 8. -- ○ Experimental laboratory angular distributions of I_2F , ClIF and HI produced from the reactions $F_2 + I_2$, ICl and HI at collision energies of 12.9, 17.4 and 16.1 kcal/mole, respectively; -- best fit laboratory angular distributions calculated by transforming $I_{c.m.}(\theta, u)$ (figures 5-7) to the laboratory frame using a full range of Newton diagrams, and then summing over laboratory velocities.

Fig. 9. -- □ Experimental laboratory velocity distribution of I_2F produced in the reaction $F_2 + I_2$ at a collision energy of 12.9 kcal/mole at four laboratory angles; -- laboratory velocity distribution derived from the centre-of-mass product distribution shown in figure 5.

Fig. 10. -- ● Product recoil energy distributions for I_2F , ClIF and HIF produced in the reaction $F_2 + I_2$, ICl and HI at collision energies of 12.9, 17.4 and 16.1 kcal/mole, respectively, obtained by angle averaging $I_{c.m.}(\theta, E_T')$. Vertical dashed line represents the approximate kinematic recoil energy limit.

Fig. 11. -- ○ Centre-of-mass angular distributions of I_2F , ClIF and HIF produced in the reactions $F_2 + I_2$, ICl and HI at collision energies of 12.9, 17.4 and 16.1 kcal/mole, respectively, obtained by averaging $I_{c.m.}(\theta, E_T')$ over recoil energy, for centre-of-mass angles $\theta \leq 180$;

□ corresponding centre-of-mass angular distributions for centre-of-mass angles $\theta \geq 180$, plotted for $2\pi - \theta$; -- smoothed centre-of-mass angular distribution representing the smoothed average of each set of points.

Fig. 12. -- Schematic energy diagram showing the stabilities of the XIF, X = I, Cl, CH₃ and H trihalogens and pseudo-trihalogens. All energies are in kcal/mole with respect to the separated atoms shown at the top.

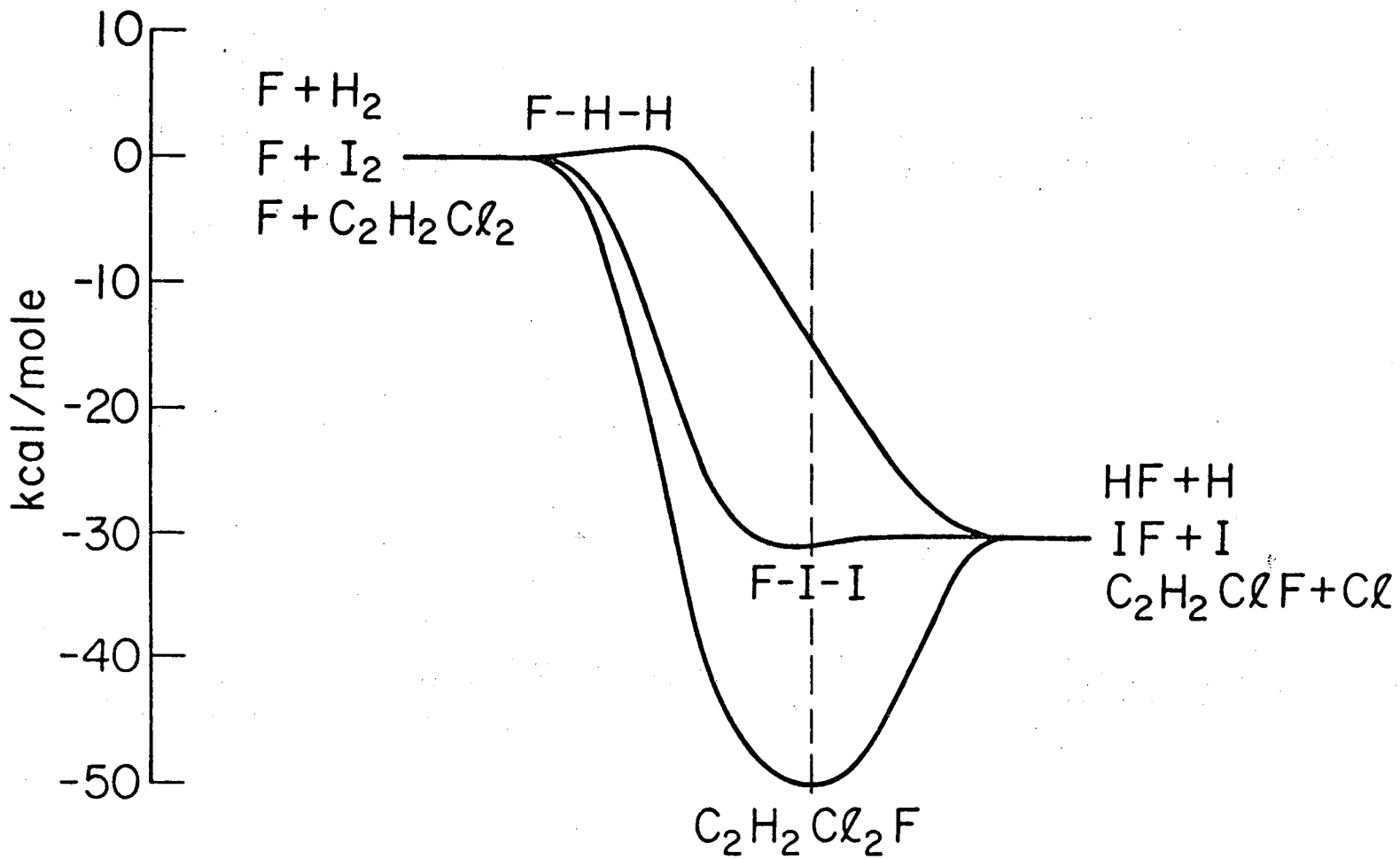


Fig. 1

XBL7511-8665

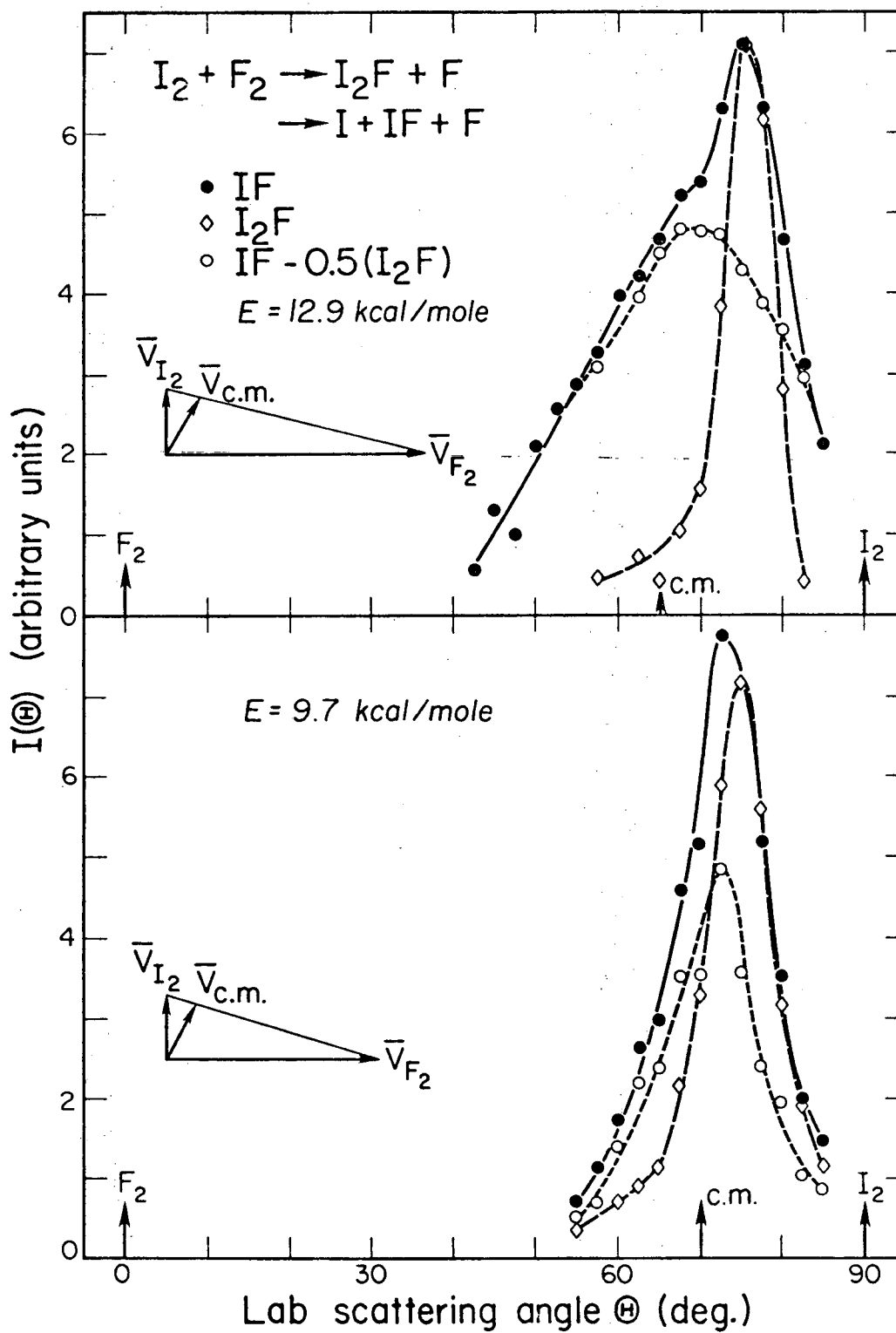
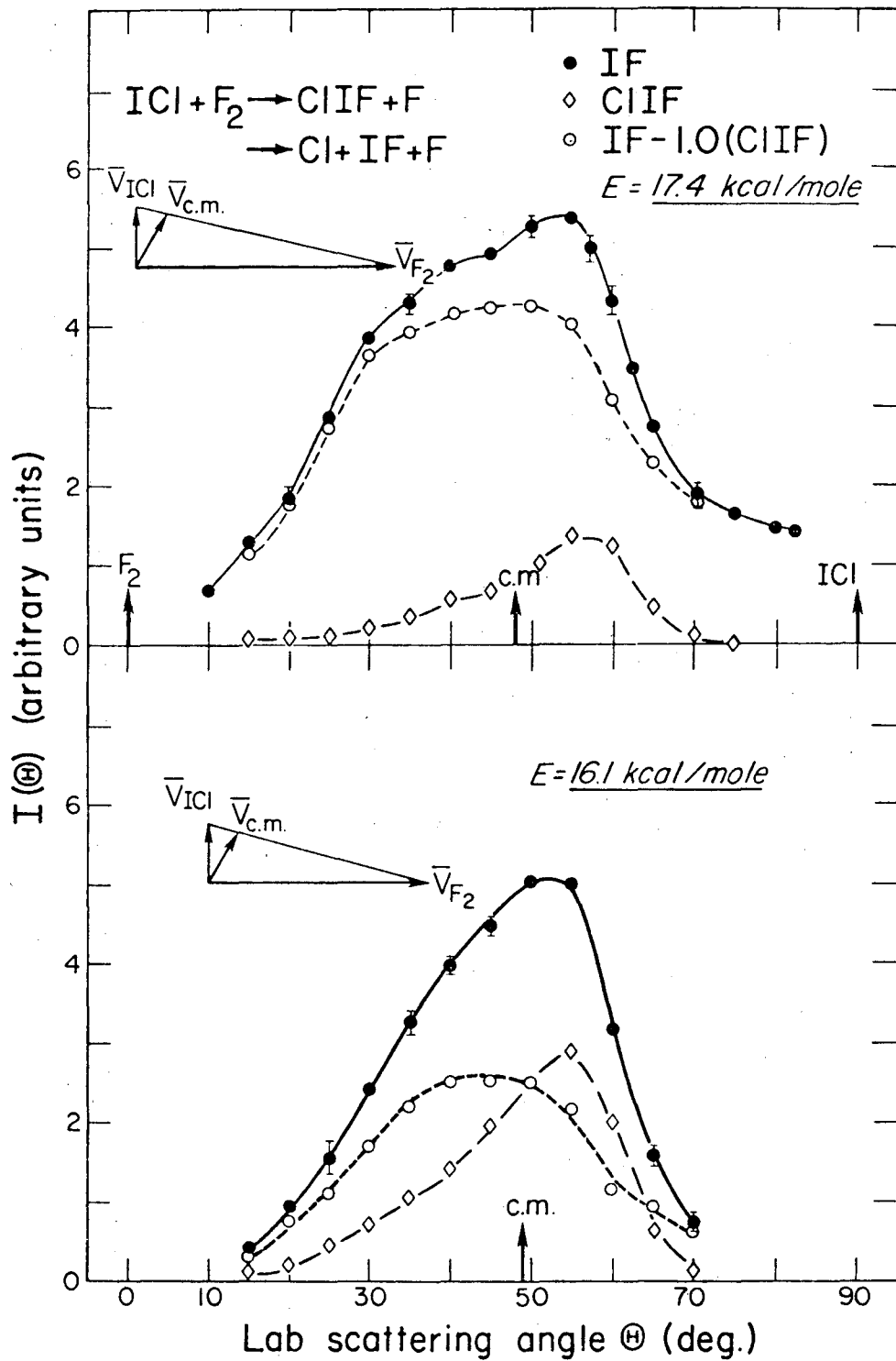


Fig. 2

XBL 7510-8536



XBL 764-2668

Fig. 3

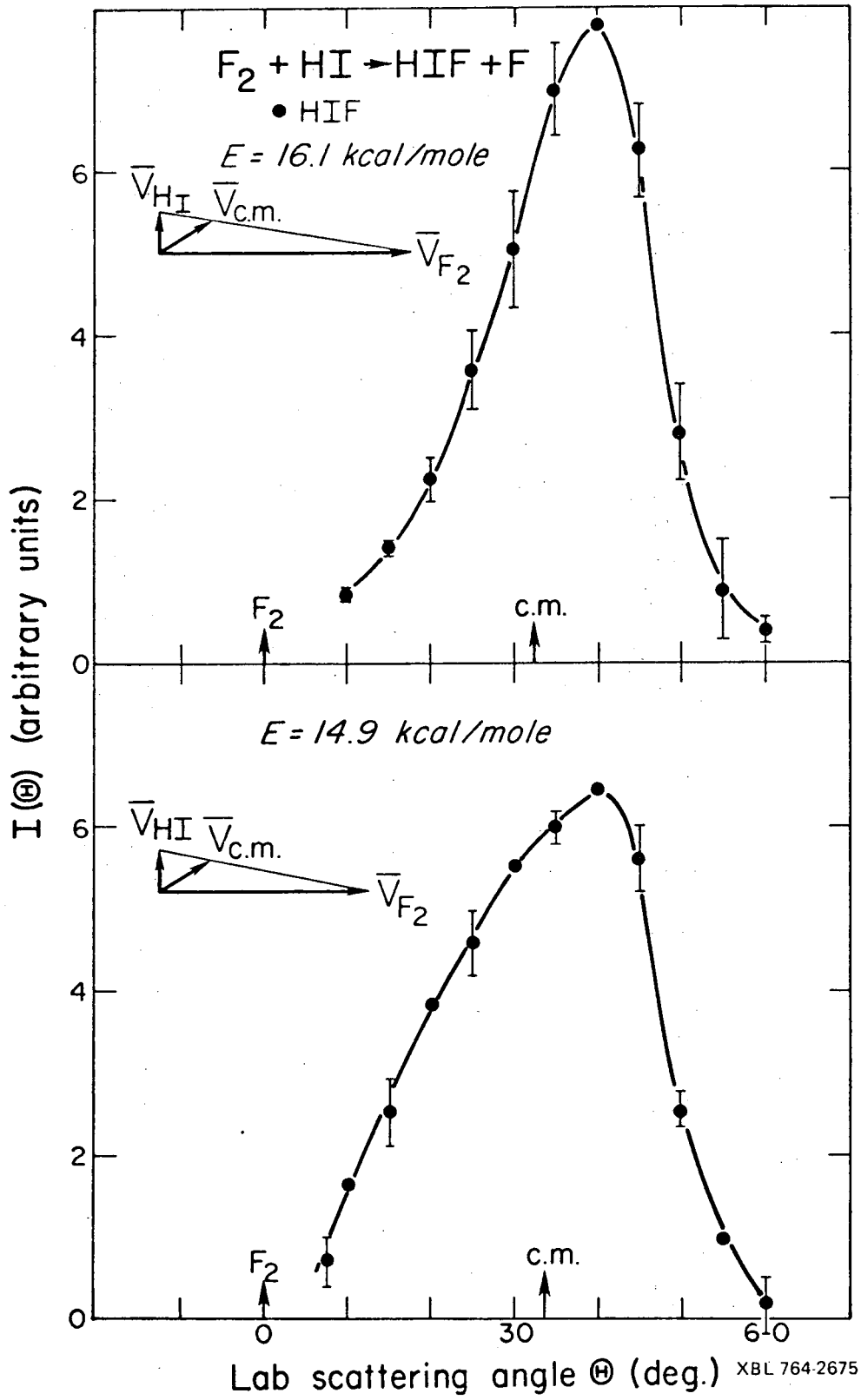
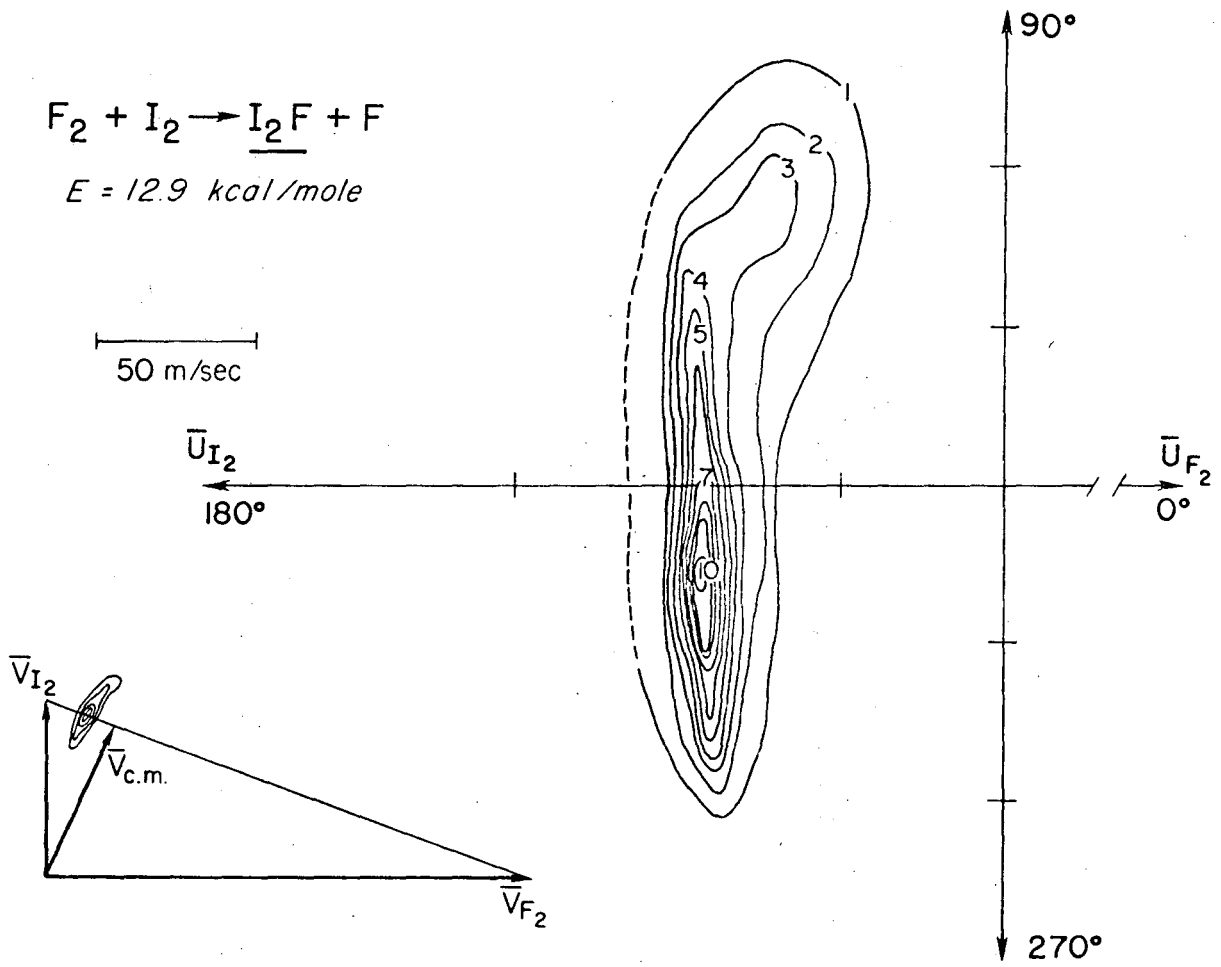
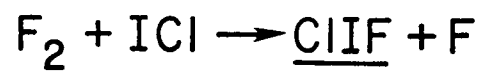


Fig. 4



XBL 764-2680

Fig. 5



$E = 17.4 \text{ kcal/mole}$

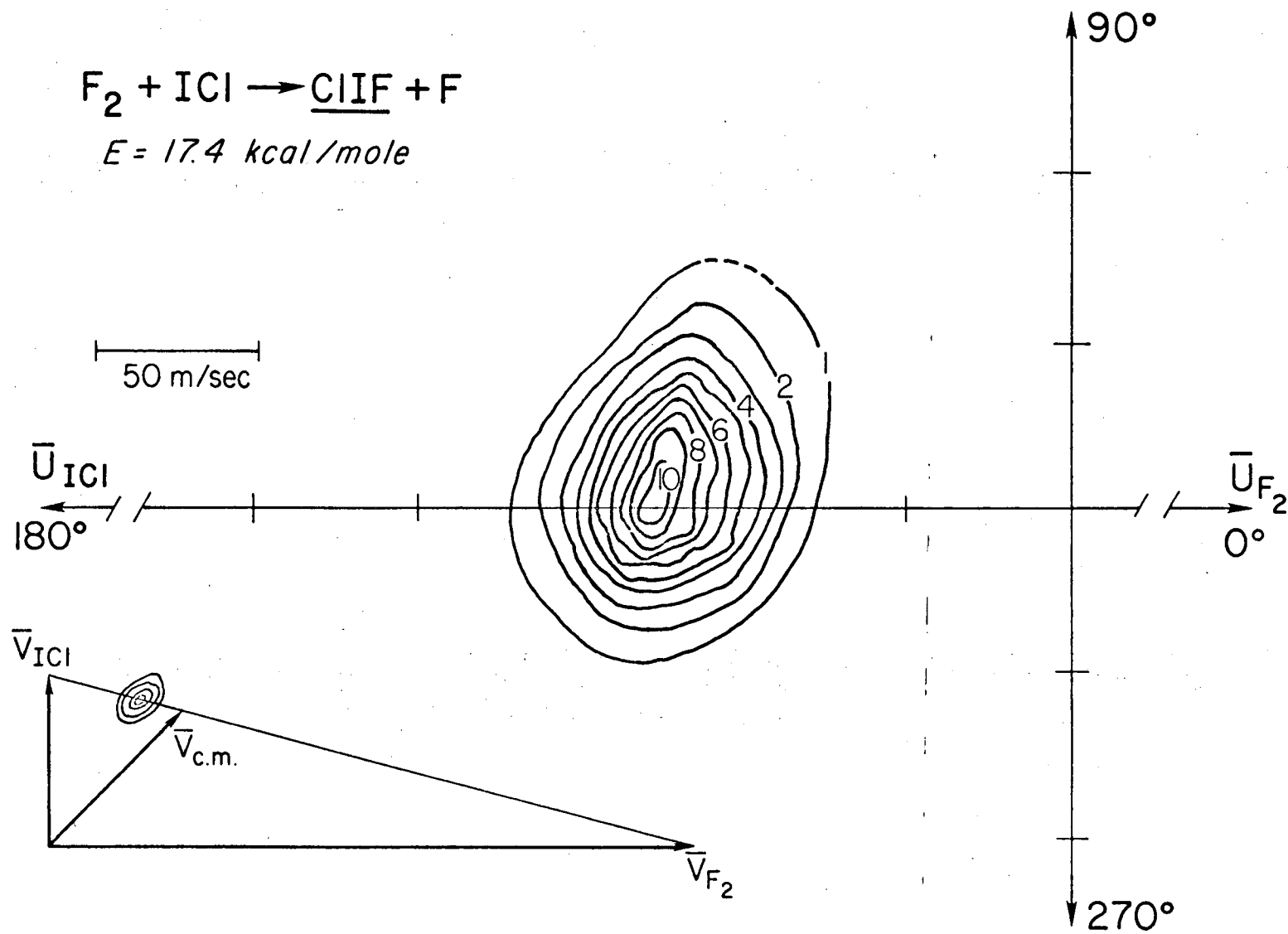
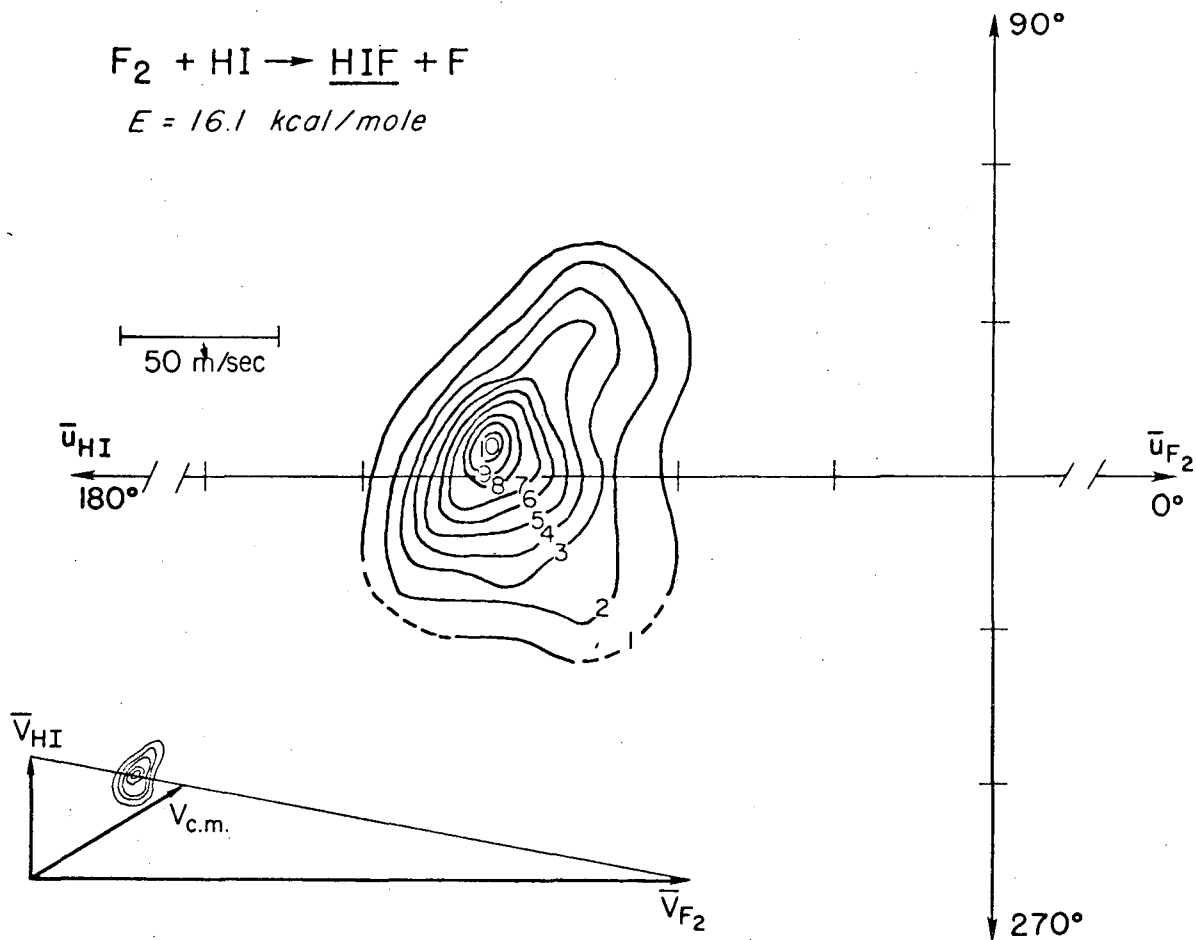


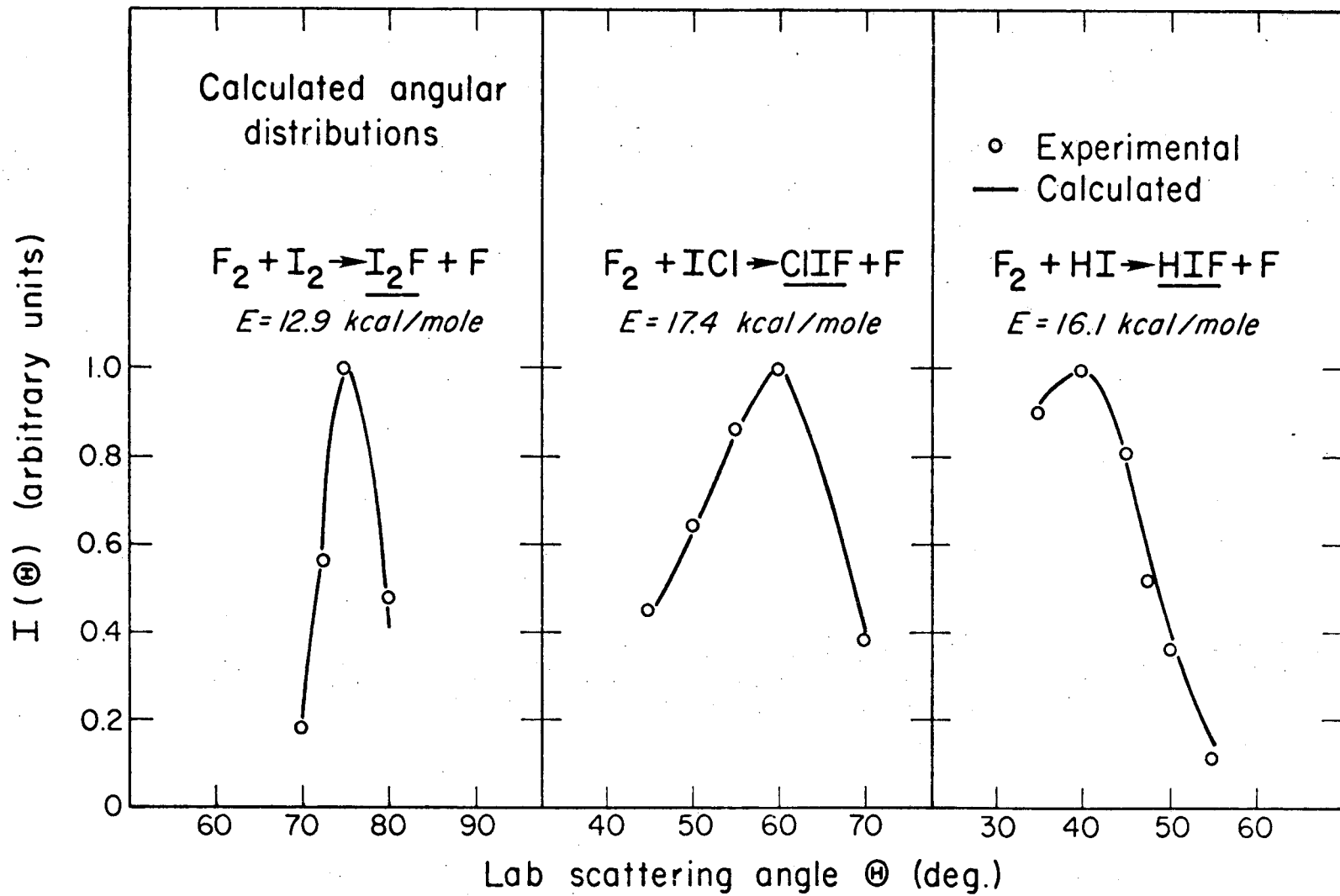
Fig. 6

XBL 764-2678



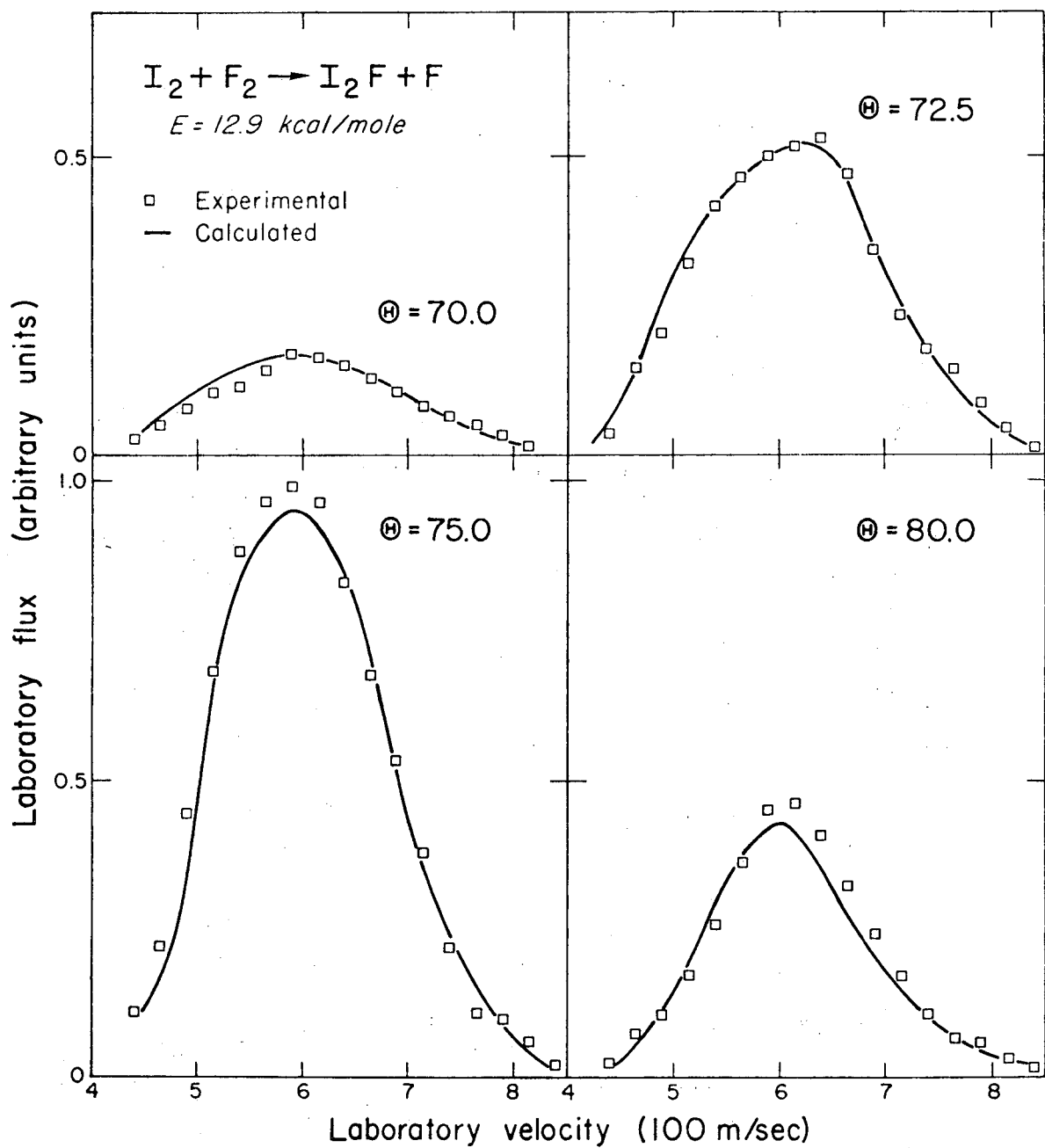
XBL 764-2681

Fig. 7



XBL 764-2677

Fig. 8



XBL 764-2679

Fig. 9

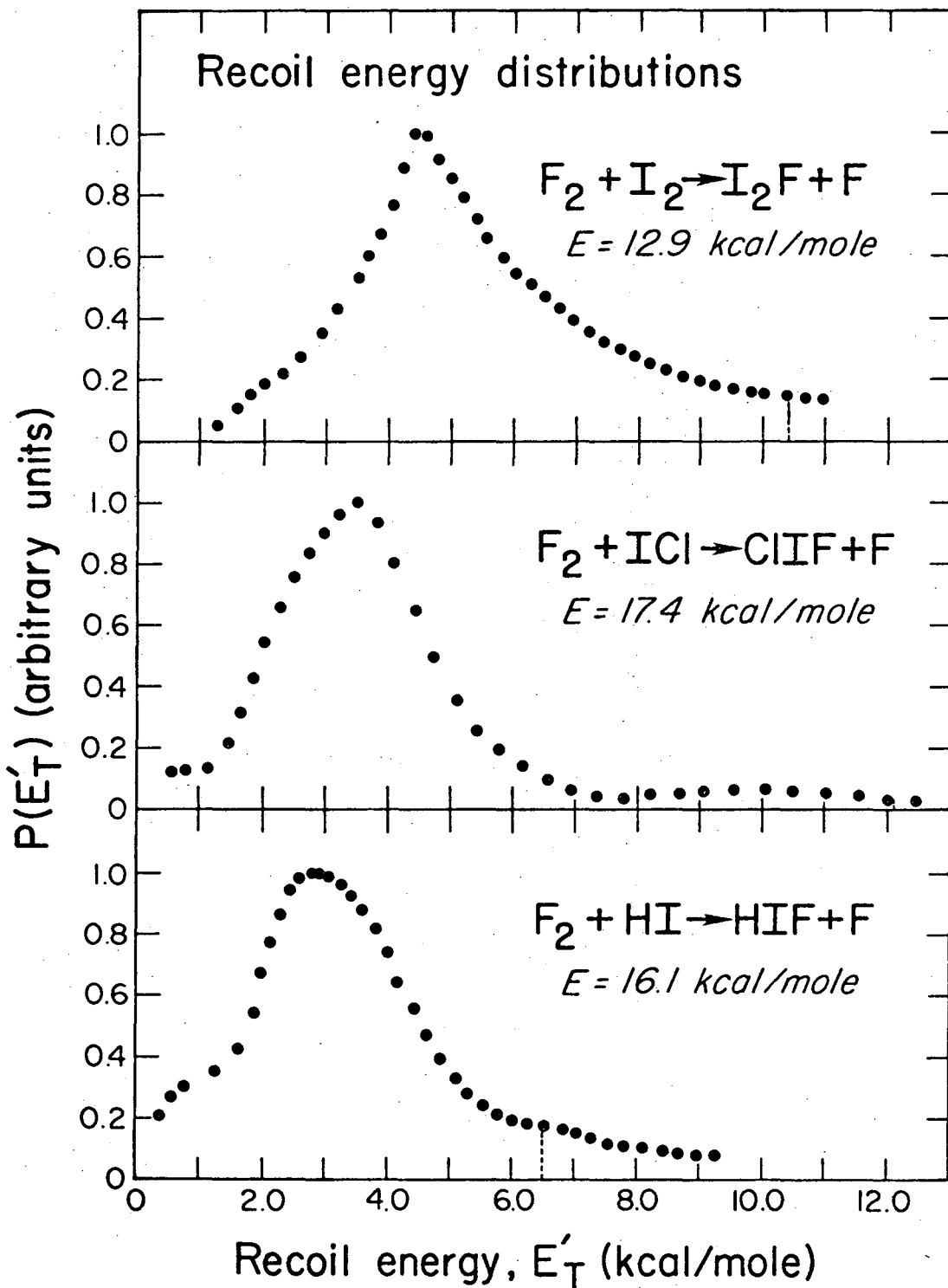


Fig. 10

XBL 764-2669

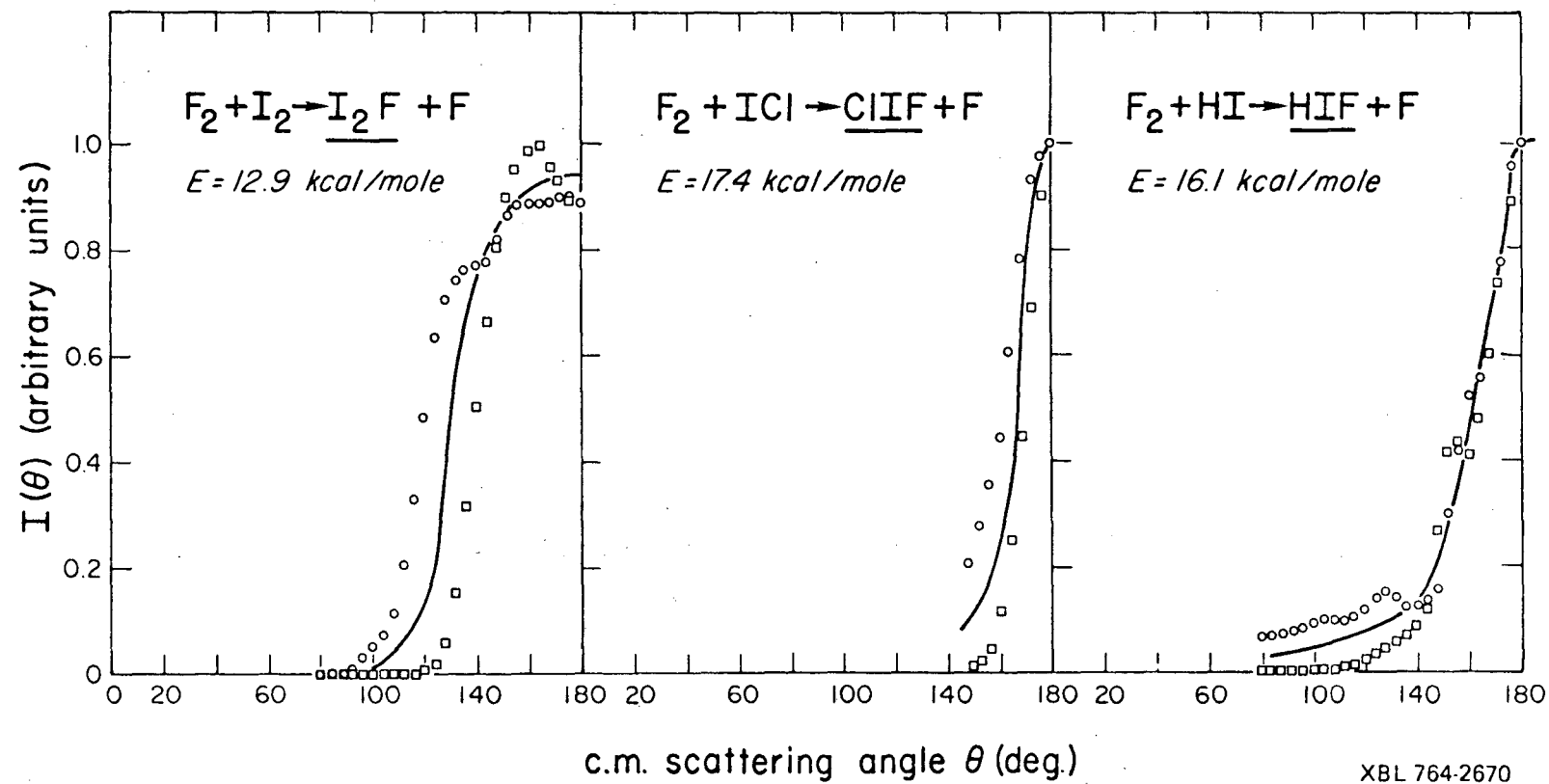
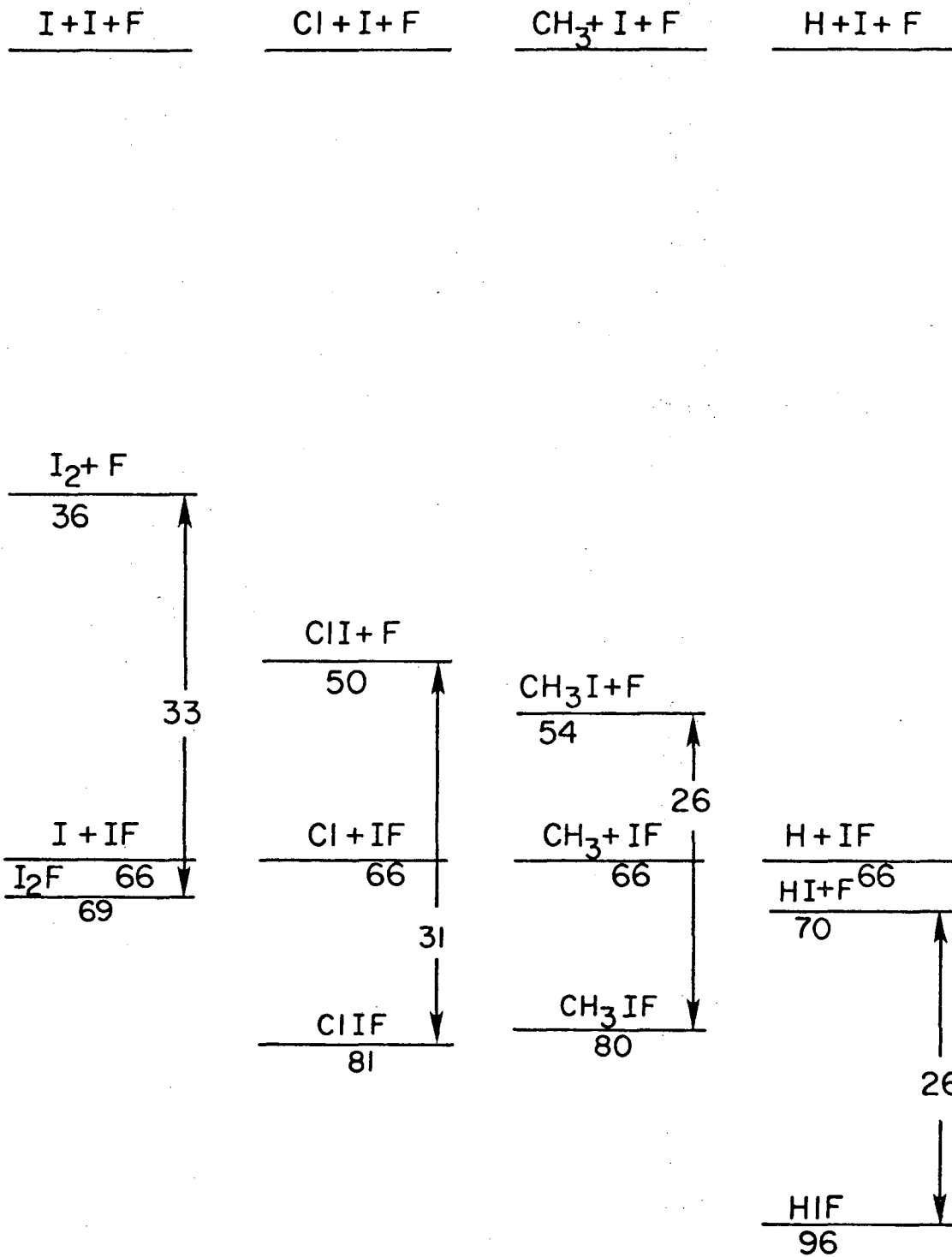


Fig. 11



XBL 764-2676

Fig. 12

LEGAL NOTICE

This report was prepared as an account of work sponsored by the United States Government. Neither the United States nor the United States Energy Research and Development Administration, nor any of their employees, nor any of their contractors, subcontractors, or their employees, makes any warranty, express or implied, or assumes any legal liability or responsibility for the accuracy, completeness or usefulness of any information, apparatus, product or process disclosed, or represents that its use would not infringe privately owned rights.

TECHNICAL INFORMATION DIVISION
LAWRENCE BERKELEY LABORATORY
UNIVERSITY OF CALIFORNIA
BERKELEY, CALIFORNIA 94720